

Cite this: *CrystEngComm*, 2012, 14, 6252–6256

www.rsc.org/crystengcomm

PAPER

Posner's cluster revisited: direct imaging of nucleation and growth of nanoscale calcium phosphate clusters at the calcite-water interface

Lijun Wang,^{*a} Shiyun Li,^a Encarnación Ruiz-Agudo,^b Christine V. Putnis^{*c} and Andrew Putnis^c

Received 2nd May 2012, Accepted 2nd July 2012

DOI: 10.1039/c2ce25669j

Although many *in vitro* studies have looked at calcium phosphate (Ca–P) mineralization, they have not emphasized the earliest events and the pathway of crystallization from solvated ions to the final apatitic mineral phase. Only recently has it become possible to unravel experimentally the processes of Ca–P formation through a cluster-growth model. Here we use mineral replacement reactions by the interaction of phosphate-bearing solutions with calcite surfaces in a fluid cell of an atomic force microscope (AFM) and reveal that the mineral surface-induced formation of an apatitic phase proceeds through the nucleation and aggregation of nanosized clusters with dimensions similar to those of Posner's clusters, which subsequently form stable amorphous calcium phosphate (ACP) plates prior to the transformation to the final crystalline phase. Our direct AFM observations provide evidence for the existence of stable Posner's clusters even though no organic template is applied.

Introduction

During the synthesis of hydroxyapatite (HAP) crystals through the interaction of calcium and phosphate ions in neutral to basic solutions, a precursor amorphous calcium phosphate phase (ACP) is formed that is structurally and chemically distinct from HAP.^{1,2} For the formation pathway of Ca–P phases in solutions or on surfaces, a cluster-growth model has been proposed and debated for decades.³ The constancy in their chemical composition over a relatively wide range of chemical preparation conditions and chemical analysis of the precursor phase indicated that this noncrystalline phase is a hydrated calcium phosphate ($\text{Ca}_3(\text{PO}_4)_2 \cdot x\text{H}_2\text{O}$) with a Ca/P ratio of 1.50, consisting of roughly spherical $\text{Ca}_9(\text{PO}_4)_6$ so-called "Posner's clusters" (PC) close-packed to form larger spherical particles with water in the interstices.³ Simulations of the peak distribution have been made regarding the particle size of Ca–P clusters and their prevalence confirmed that particles ranging in size from 0.8 to 1.0 nm are likely to exist as clusters in simulated body fluid.⁴ Ca–P clusters, from which HAP crystals can be constituted, must form in solutions as HAP grows.⁴ However, such nanometer-sized clusters as building blocks for ACP and subsequent transformation to HAP are difficult to visualize directly. Very recently, Dey *et al.* used a Langmuir monolayer of arachidic acid to mimic biological Ca–P mineralization, and they observed clusters with an average diameter of 0.87 ± 0.2 nm

during the earliest stages of nucleation using high-resolution cryogenic transmission electron microscopy (HR-cryoTEM).⁵ Despite the significance of this study, the formation pathway of Ca–P phases in the absence of organic templates has never been directly observed, and thus the role of nanosized clusters formed on mineral surfaces and their connection to larger aggregates remain largely unknown.

Recently, it has been shown that solvent-mediated mineral replacement reactions involve an interface-coupled mechanism of the dissolution of a solid in an aqueous fluid and the subsequent precipitation of a new, thermodynamically more stable solid phase that replaces the parent solid.^{6,7} Using this novel strategy of re-equilibration of solids in the presence of a fluid phase, various Ca–P materials have been formed by the replacement of different calcium carbonate polymorphs.^{8,9} In this work, we follow the earliest stages of the formation of Ca–P phases resulting from the interaction of phosphate-bearing solutions with a calcite surface in a fluid cell of an atomic force microscope (AFM), without the support of an organic template, by adjusting the concentration of $(\text{NH}_4)_2\text{HPO}_4$ solutions to control the nucleation rates. We observe that the formation of Ca–P phases assisted by calcite surfaces is initiated by the aggregation of clusters that leads to the formation of ACP, which finally transforms into crystalline HAP.

Experimental

In situ dissolution experiments were performed using a Digital Instruments Nanoscope IIIa AFM working in contact mode. The scanning frequency was *ca.* 3 Hz with an average scan time 1.5 min per scan. Iceland Spar fragments (*ca.* $3 \times 3 \times 1$ mm in size) were freshly cleaved before each dissolution experiment, and $\{10\bar{1}4\}$ calcite surfaces were exposed to the solutions in an O-ring-sealed

^aCollege of Resources and Environment, Huazhong Agricultural University, Wuhan 430070, China. E-mail: ljwang@mail.hzau.edu.cn; Fax: (+)86-27-87288095

^bDepartment of Mineralogy and Petrology, University of Granada, Granada, 18071, Spain

^cInstitut für Mineralogie, University of Münster, 48149, Münster, Germany. E-mail: putnisc@uni-muenster.de; Fax: (+)49-251-8338397

fluid cell. Di-ammonium phosphate ((NH₄)₂HPO₄) solutions of concentration ranging from 5 to 50 mM were passed through the fluid cell. In another set of experiments, monosodium citrate (1–10 μM) was added to a 50 mM phosphate solution to study the effect of this additive as a stabilizer of nano-sized Ca–P particles. The pH values of (NH₄)₂HPO₄ solution in the absence and presence of citrate were adjusted to pH 7.9 ± 0.2. All experiments were performed under ambient conditions (22 ± 1 °C and partial pressure CO₂ ~ 10^{-3.5} atm.). Reaction solutions were prepared from high-purity solids, (NH₄)₂HPO₄, and monosodium citrate dissolved in doubly-deionized water (resistivity > 18 mΩcm⁻¹). Each of the solutions was gradually passed over the calcite surface at a constant flow rate *ca.* 50 mL h⁻¹ using a syringe pump connected with vinyl tubes. The chosen flow rate was enough to ensure a surface-controlled reaction rather than diffusion control.¹⁰ Experiments were repeated at least twice to ensure reproducibility of the results. The AFM images and the cluster heights were analyzed using the NanoScope (Version 5.12b48) and WSxM 5.0 (Develop 4.1) software.¹¹

HAP cluster (Posner) model was visualized using the Cerius² (version 4.0) graphical molecular modeling program (Accelrys formerly MSI). Symmetry and co-ordination information was used from Yin and Stott (2003)¹² and Kanzaki *et al.* (2001).¹³

Results and discussion

In situ AFM monitoring of slow crystallization processes provides a unique opportunity to observe the nucleation and growth of Ca–P clusters as shown in Fig. 1. Prior to the input of the reaction solutions, the calcite (10 $\bar{1}$ 4) cleavage face was exposed to deionized water in the fluid cell of an AFM. Dissolution immediately occurred with the formation of typical rhombohedral etch pits on the exposed surfaces. The known orientation of the etch pits in pure water was used to establish the crystallographic orientation of the seed substrates.¹⁴ Following the injection of 10–50 mM (NH₄)₂HPO₄ solutions at constant pH 7.9 and 25 °C, the etch pits changed from the characteristic rhombohedral morphology to fan-shaped (Fig. 1a). The dissolution of calcite in the presence of (NH₄)₂HPO₄ solutions provided a source of Ca²⁺ ions, which resulted in supersaturation of the interfacial fluid with respect to a Ca–P phase and its nucleation on the dissolving calcite surface. High-resolution AFM demonstrated that the observed clusters were present partially as isolated entities with a height of 1.02 ± 0.1 nm (Arrow 1 in Fig. 1a) or small spherical aggregates (2.13 ± 0.2 nm, Arrow 2 in Fig. 1a) at the earliest stages of Ca–P nucleation. The individual clusters were slightly larger than previously reported sizes (0.7–1.0 nm)⁴ as well as the theoretical value of Posner's clusters (~0.95 nm).⁵ Cross-sectional analysis of the growing plates is shown in Fig. 1b–d. The observed clusters subsequently spread laterally to form 2-D plates over a time period of 135, 269, and 403 s with a height of 2.22 ± 0.2, 2.05 ± 0.2, and 2.17 ± 0.2 nm, respectively.

Recent results have shown that in the early nucleation stage, citrate can partly bind to ACP clusters, and in the later growth stage such strongly bound citrate molecules can stabilize the apatite nanocrystals during bone biomineralization.^{15,16} To test this effect, 10 μM monosodium citrate was added to the 50 mM (NH₄)₂HPO₄ solution at pH 7.9. In the presence of citrate, Ca–P

nucleation was delayed and occurred only after about 50 min of the input of reaction solutions. However, a larger number of clusters with a narrower size distribution (ranging from 1.0 to 2.0 nm, Fig. 2b) formed with a slightly preferred nucleation site along macro-step edges parallel to the $\bar{4}$ 41 direction (Fig. 2a). They were stabilized by citrate that seemed to inhibit their aggregation to form 2D plates on the calcite (10 $\bar{1}$ 4) cleavage face compared to aggregation in the absence of citrate (Fig. 1b–d). All clusters were loose aggregates, and they subsequently fused further by a closer stacking (Fig. 3). When the scanning of the surface was stopped for 3 h after the injection of a 50 mM of (NH₄)₂HPO₄ solution, further growth leading to the formation of denser 2-D plates was observed (Fig. 4). These layers, formed at the early stages of the reaction, were characterized using Raman spectroscopy and they were found to be ACP, which further develops to form poorly crystalline HAP by an Ostwald ripening process¹⁷ as shown in our recent work.¹⁸

The time dependence of Ca–P nucleation on calcite is consistent with an observed growth model having an average constant nucleation rate before the subsequent evolution of the individual clusters.¹⁸ Even though this growth model is simple, it nevertheless provides a good fitting of kinetic data for the early growth stages.¹⁸ The narrow cluster-size distribution is important for understanding 2-D plate uniformity (similar height during coalescence) (Fig. 1b–d). A slow, diffusion-limited growth process is expected due to the reduction in the supply of Ca ions from calcite surfaces as a result of the almost complete coverage of the reacting surface by the deposition of Ca–P plates (Fig. 4a). The growth rate of Ca–P plates was not expected to drop to zero because some release of Ca ions from the non-covered areas of the dissolving calcite substrate, marked by an arrow in Fig. 4a, still existed, and the thickness increased up to a final value of about 3.44 nm (Fig. 4b).

Ca–P is highly polymorphic in that it can exist in different crystal structures. The first polymorph formed after nucleation is often ACP, which subsequently crystallizes.² ACP has no long-range order, but it often has short-range structural order that determines the crystal structure following crystallization.² Our *in situ* AFM observations clearly demonstrate that the precipitation of HAP plates on calcite involves the formation and aggregation of nanosized clusters which serve as building blocks for ACP plates, which subsequently transform into the final HAP phase, either through a dissolution-recrystallization process² or a solid-state transition.¹⁹ Our direct observations also confirm the existence of stable clusters even though no organic template (possible control of organic surfaces on inorganic crystallization) was present. The observed clusters were amorphous or of low structural order, and it is important to understand how they were able to remain relatively stable for a sufficiently long period of time so that the dense stacking/packing and the fusion to form ACP could occur. In a study of calcium carbonate nucleation, long-lived precritical clusters (about 2 nm in diameter) have been observed, and they grow by colliding and coalescing.²⁰ If metastable precritical clusters exist in solution before nucleation,^{20,21} they must lie in a free energy minimum, although their structure and depth remain unknown.²² Furthermore, if clusters were stable with respect to the solution state, they would be expected to grow larger, which is not observed. They coalesce. This may be explained if the clusters represent dynamic solution

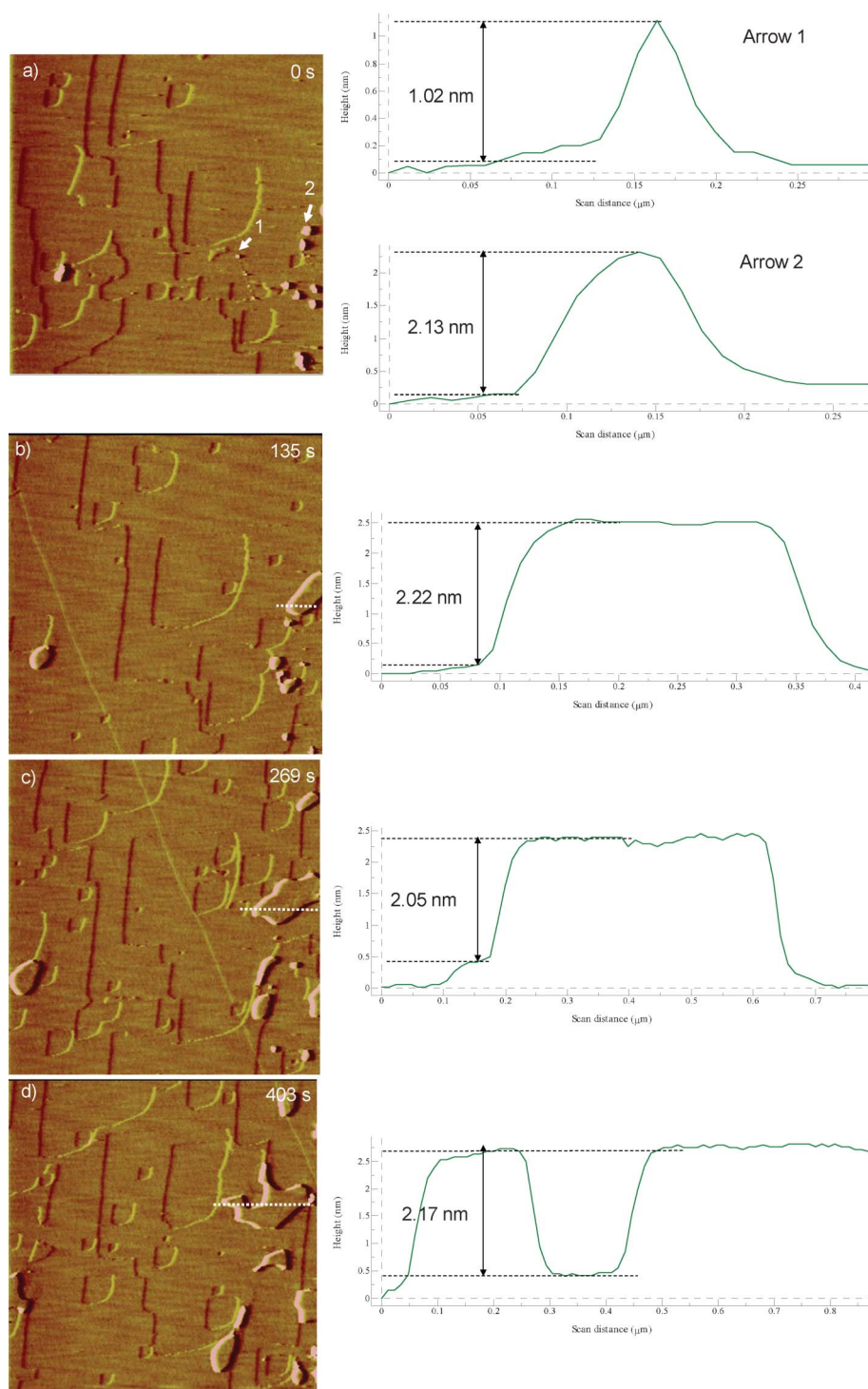


Fig. 1 Sequential AFM deflection images and cross-sectional analyses of initially forming Ca-P clusters and their developing growth on calcite {10 $\bar{1}$ 4} cleavage face. AFM images a-d, 3 × 3 μ m.

species, which are not nucleated, as proposed by Demichelis *et al.*²³ That is, their maximum size may be determined by the rate of growth, which is diffusion limited, *versus* the rate of ion loss.²³ Following this notion, the coalescence of clusters may be the actual nucleation step. However, it is difficult to determine whether these clusters are nucleated, although our AFM observations suggest this as a possible nucleation step.

The formation of these clusters may also help to lower the activation barriers for crystal nucleation and growth of the metastable polymorphs of Ca-P phases. Once such metastable crystals grow, a separate set of nucleation events and/or a dissolution-precipitation mechanism corresponding to the pH changes may be required to form a subsequently more stable phase. However, at present there is no definitive evidence

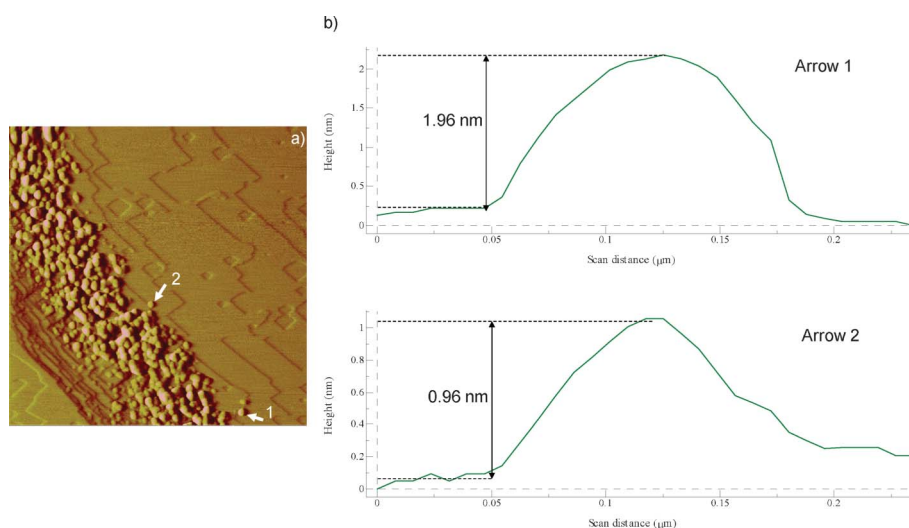


Fig. 2 (a) AFM image and (b) cross-sectional analyses of stabilized Ca–P clusters with narrow size distributions on calcite after injecting reaction solutions in the presence of citrate. Image a, $4 \times 4 \mu\text{m}$.

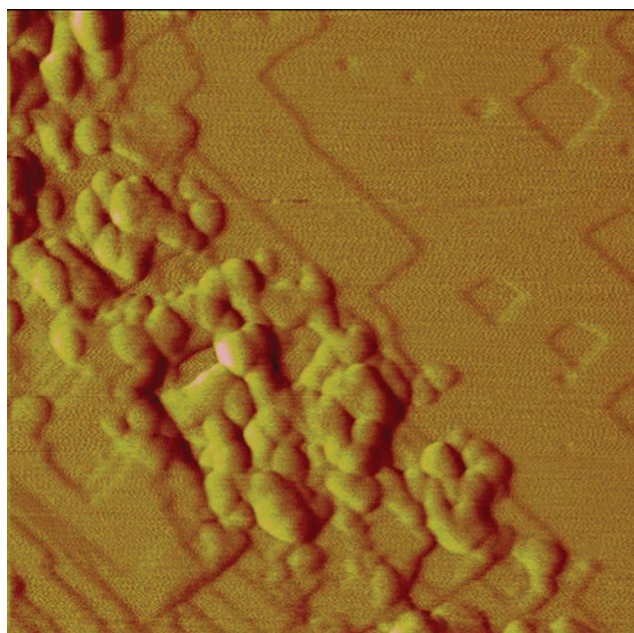


Fig. 3 AFM image of loose aggregates of Ca–P clusters. Image, $2 \times 2 \mu\text{m}$.

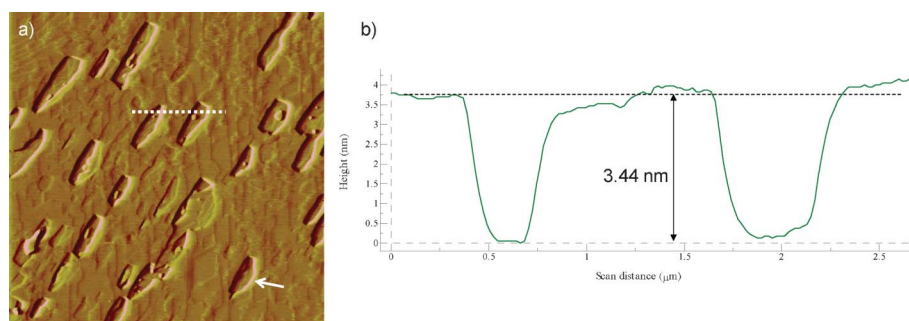


Fig. 4 (a) AFM Image of the ACP plates formed by the subsequent fusion of clusters and (b) cross-sectional analyses of the height of 2-D plates along a dotted line. An arrow in Fig. 4a shows an irregular hole on the dissolving substrate of calcite. Image a, $10 \times 10 \mu\text{m}$.

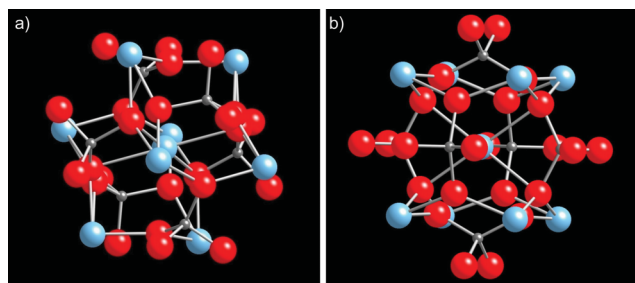


Fig. 5 Graphical representation of a Posner's cluster with composition $\text{Ca}_9(\text{PO}_4)_6$ and a diameter of about 0.86 nm. (a) top view and (b) side view. Atom colouring scheme: calcium, blue; phosphorus, gray; oxygen, red.

particular, it is suggested that the chirality of PCs found in the HAP environment does not exist in an isolated form and in aqueous solution. Posner speculated that clusters may play a role during nucleation and growth of Ca–Ps, especially HAP, which was observed experimentally by Dey *et al.*⁵ However, it is still not known whether the structure of these clusters in a supersaturated solution is the same as in the bulk Ca–P phase, based only on an agreement in size we have observed.

The reconsideration of PCs as possible components of the actual structure of ACP resulted from the cluster growth model of the HAP crystal.⁴ *Ab initio* calculations confirmed that stable isomers exist on the $[\text{Ca}_3(\text{PO}_4)_2]_3$ potential energy surface (PES).¹³ These isomers correspond to compact arrangements, *i.e.*, arrangements in which the Ca and PO_4 are positioned closely together. Their geometries are compatible with the term “roughly spherical” used in Posner's hypothesis. The observed particle size distribution of clusters formed in the $\text{CaCl}_2\text{--H}_3\text{PO}_4\text{--KCl--H}_2\text{O}$ system was also centered at about 0.8–1.0 nm, and the clusters with Ca/P ratios in the range 1–8 remained stable for at least 100 h.^{30,31} Using computational chemistry techniques,²⁸ the calculated energy per unit monomer reaches a minimum value for a three-unit cluster ($[\text{Ca}_3(\text{PO}_4)_2]_n$, $n = 3$). These structures generally become energetically more stable during the actual crystal growth process; the existence of Ca–P clusters acting as HAP growth units seems highly likely. Regarding the unit cells of apatite crystal structures projected on the *ab*-plane, they appear to be $\text{Ca}_9(\text{PO}_4)_6$ clusters of size 0.815 nm along the *a*-axis and 0.87 nm along the *c*-axis.³¹ This suggests the Ca/P ratio of apatite gradually increases toward the stoichiometric ratio of 1.67 after the crystal has been formed, and this cluster growth model postulates that the clusters stack along the *c*-axis.³¹

Conclusions

We have observed the nucleation and growth of individual, nanoscale Ca–P clusters using *in situ* AFM that allows real-time observation of cluster growth at the solid–fluid interface during the interaction of phosphate-bearing solutions with calcite surfaces in a fluid cell. The mineral surface-assisted formation of Ca–P phases may proceed through the aggregation of metastable clusters, rather than by addition of ions or molecules to a nucleus, and subsequently form stable ACP plates prior to the transformation to the final crystalline phase. The important effect of organic additives such as citrate on stabilizing Ca–P nanosized clusters at the earliest stages of nucleation has also been recognized. This

direct imaging and analysis at the solid–fluid interface is essential to capture nanoscale clusters and to gain a deeper understanding of the early events of Ca–P crystallization.

Acknowledgements

This work was supported by the National Natural Science Foundation of China (Grant No. 41071208) and a startup grant from the Huazhong Agricultural University (52204-09008) to Lijun Wang. E. R-A acknowledges a Ramón y Cajal grant from Spanish Ministry of Economy and Competitiveness as well as funding from the project P11-RNM-7550 and the research group RNM179 (Junta de Andalucía). Experimental facilities in the Institut für Mineralogie, Münster are supported by the Deutsche Forschungsgemeinschaft (DFG). We also thank Dr Helen King for support for the computer model of the cluster.

References

- 1 E. D. Eanes, H. Gillissen and A. S. Posner, *Nature*, 1965, **208**, 365–367.
- 2 L. J. Wang and G. H. Nancollas, *Chem. Rev.*, 2008, **108**, 4628–4669.
- 3 A. S. Posner and F. Betts, *Acc. Chem. Res.*, 1975, **8**, 273–281.
- 4 K. Onuma and A. Ito, *Chem. Mater.*, 1998, **10**, 3346–3351.
- 5 A. Dey, P. H. H. Bomans, F. A. Muller, J. Will, P. M. Frederik, G. de With and N. A. J. M. Sommerdijk, *Nat. Mater.*, 2010, **9**, 1010–1014.
- 6 A. Putnis, *Rev. Mineral. Geochem.*, 2009, **70**, 87–124.
- 7 A. Putnis and C. V. Putnis, *J. Solid State Chem.*, 2007, **180**, 1783–1786.
- 8 C. M. Zaremba, D. E. Morse, S. Mann, P. K. Hansma and G. D. Stucky, *Chem. Mater.*, 1998, **10**, 3813–3824.
- 9 A. Kasiotas, T. Geisler, C. Perdikouri, C. Trepmann, N. Gussone and A. Putnis, *Geochim. Cosmochim. Acta*, 2011, **75**, 3486–3500.
- 10 Y. Liang, D. R. Baer, J. M. McCoy, J. E. Amonette and J. P. LaFemina, *Geochim. Cosmochim. Acta*, 1996, **60**, 4883–4887.
- 11 I. Horcas, R. Fernandez, J. M. Gomez-Rodriguez, J. Colchero, J. Gomez-Herrero and A. M. Baro, *Rev. Sci. Instrum.*, 2007, **78**, 013705.
- 12 X. L. Yin and M. J. Stott, *J. Chem. Phys.*, 2003, **118**, 3717–3723.
- 13 N. Kanzaki, G. Treboux, K. Onuma, S. Tsutsumi and A. Ito, *Biomaterials*, 2001, **22**, 2921–2929.
- 14 L. J. Wang, E. Ruiz-Agudo, C. V. Putnis and A. Putnis, *CrystEngComm*, 2011, **13**, 3962–3966.
- 15 Y. Y. Hu, A. Rawal and K. Schmidt-Rohr, *Proc. Natl. Acad. Sci. U. S. A.*, 2010, **107**, 22425–22429.
- 16 B. Q. Xie and G. H. Nancollas, *Proc. Natl. Acad. Sci. U. S. A.*, 2010, **107**, 22369–22370.
- 17 T. Nonoyama, T. Kinoshita, M. Higuchi, K. Nagata, M. Tanaka, K. Sato and K. Kato, *Langmuir*, 2011, **27**, 7077–7083.
- 18 L. J. Wang, E. Ruiz-Agudo, C. V. Putnis, M. Menneken and A. Putnis, *Environ. Sci. Technol.*, 2012, **46**, 834–842.
- 19 T. Tsuji, K. Onuma, A. Yamamoto, M. Iijima and K. Shiba, *Proc. Natl. Acad. Sci. U. S. A.*, 2008, **105**, 16866–16870.
- 20 D. Gebauer, A. Völkel and H. Cölfen, *Science*, 2008, **322**, 1819–1822.
- 21 E. M. Pouget, P. H. H. Bomans, J. A. A. M. Goos, P. M. Frederik, G. de With and N. A. J. M. Sommerdijk, *Science*, 2009, **323**, 1455–1458.
- 22 F. C. Meldrum and R. P. Sear, *Science*, 2008, **322**, 1802–1803.
- 23 R. Demichelis, P. Raiteri, J. D. Gale, D. Quigley and D. Gebauer, *Nat. Commun.*, 2011, **2**, 590.
- 24 A. P. Alivisatos, *Science*, 2000, **289**, 736–737.
- 25 D. Gebauer and H. Cölfen, *Nano Today*, 2011, **6**, 564–584.
- 26 J. L. Banfield, S. A. Welch, H. Zhang, T. T. Ebert and R. L. Penn, *Science*, 2000, **289**, 751–754.
- 27 A. Navrotsky, *Proc. Natl. Acad. Sci. U. S. A.*, 2004, **101**, 12096–12101.
- 28 G. Treboux, P. Layrolle, N. Kanzaki, K. Onuma and A. Ito, *J. Phys. Chem. A*, 2000, **104**, 5111–5114.
- 29 G. Treboux, P. Layrolle, N. Kanzaki, K. Onuma and A. Ito, *J. Am. Chem. Soc.*, 2000, **122**, 8323–8324.
- 30 A. Oyane, K. Onuma, T. Kokubo and A. Ito, *J. Phys. Chem. B*, 1999, **103**, 8230–8235.
- 31 K. Onuma, *Prog. Cryst. Growth Charact. Mater.*, 2006, **52**, 223–245.